COPY

Naval Research Laboratory

Washington, DC 20375-5000

NRL Memorandum Report 6756

AD-A231 586

Transverse Klystron

Y. SEO* AND P. SPRANGLE

Beam Physics Branch
Plasma Physics Division

**FM Technologies, Inc.,*
Fairfax, VA 22032

January 31, 1991

91 2 04 134

REPORT DOCUMENTATION PAGE

Form Approved
OMB No. 0704-0188

1. AGENCY USE ONLY (*Leave blank*)	2. REPORT DATE	3. REPORT TYPE AND DATES COVERED
	1991 January 31	Interim

4. TITLE AND SUBTITLE
Transverse Klystron

5. FUNDING NUMBERS
JO #47-0899-0-1

6. AUTHOR(S)
Y. Seo* and P. Sprangle

7. PERFORMING ORGANIZATION NAME(S) AND ADDRESS(ES)
Naval Research Laboratory
Washington, DC 20375-5000

8. PERFORMING ORGANIZATION REPORT NUMBER
NRL Memorandum Report 6756

9. SPONSORING/MONITORING AGENCY NAME(S) AND ADDRESS(ES)
ONR
Arlington, VA

10. SPONSORING/MONITORING AGENCY REPORT NUMBER

11. SUPPLEMENTARY NOTES
*FM Technologies, Inc., Fairfax, VA 22032

12a. DISTRIBUTION/AVAILABILITY STATEMENT
Approved for public release;
distribution unlimited

12b. DISTRIBUTION CODE

13. ABSTRACT (*Maximum 200 words*)

An analytic solution is presented for the longitudinal density modulation of a bending magnet with a transverse scanning electron beam. The analysis is carried out for the cases with and without a guiding magnetic field. Dependence of the electron bunching on various design parameters is clarified in both cases. In the case without a guide field, the beam focusing properties, and the effects of energy spread and self-field are studied. The focusing conditions are determined and a condition for cancelling the effect of energy spread is found. It is shown, moreover, that the self-field enhances electron bunching in the bending magnet due to the negative mass effect. In the case with a guide field, a resonant excitation in the modulation cavity is considered in order to enhance the transverse modulation. A configuration with a half cusp field has also been considered to avoid the difficulty in scanning modulation in the presence of the guide field.

14. SUBJECT TERMS
scanning electron beam
drift path difference
longitudinal density modulation

15. NUMBER OF PAGES
35

16. PRICE CODE

17. SECURITY CLASSIFICATION OF REPORT	18. SECURITY CLASSIFICATION OF THIS PAGE	19. SECURITY CLASSIFICATION OF ABSTRACT	20. LIMITATION OF ABSTRACT
UNCLASSIFIED	UNCLASSIFIED	UNCLASSIFIED	SAR

NSN 7540-01-280-5500

Standard Form 298 (Rev 2-89)
Prescribed by ANSI Std Z39-18
298-102

CONTENTS

I. Introduction

Scanned beam modulation, recently proposed in the Soviet Union, suggests potentially diverse applications for generation of high power coherent radiation. An initiating impact has been made through the invention of the gyrocon and the magnicon.[1,2] Both devices utilize an electron beam deflected transversely with an RF input signal, and injected into an interaction cavity, scanning in-phase to the cavity mode. All the electrons in the beam are, thus, in the right phase with the field, ready for efficient energy transfer. The efficiency is much higher than those achieved with usual modulation schemes. For example, in usual cyclotron maser devices such as a gyrotron,[3] density modulation is obtained through the negative mass instability. Although the majority of electrons are bunched at the right phase to the interacting field, the bunching is not perfect in the sense that a small portion of the electrons remain at the reverse phase, reducing the overall efficiency. In this sense a magnicon (gyrocon) can be called a super-bunched gyrotron (klystron). This "super-bunching" is automatically obtained through the transverse modulation.

Perhaps the most important technical issue on practical application of the scanning beam will be the requirement on the beam brightness, i.e. the phase space density of electrons. A high brightness is strictly required in both the gyrocon and the magnicon scheme, and in fact, it is expected that the requirement applies to any use of scanning beams in order not to smear out the transverse modulation. Developments in various types of high brightness electron guns,[2] especially those with field emission are, thus, essential to practical utilization of scanning beams.

Manuscript approved November 1, 1990.

Once the requirement is fulfilled, scanning beams are expected to be used potentially in a variety of ways. The configuration in this paper is one example out of those varieties.

Mako and Godlove[4] recently proposed a variation of the conventional klystron which utilizes the scanning beam. They call it a transverse klystron in the sense that the beam modulation is done in the direction transverse to the electron beam propagation (scanning beam). Instead of free space drift as in the conventional klystron,[5] the modulated beam is injected into a region with a vertical magnetic field which bends the electron trajectory. On exiting from the bending magnet the electrons get bunched in its propagation direction. This longitudinal bunching is basically due to the drift path difference between modulated and equilibrium orbits. The operation frequency range is expected to be from a few hundred MHz up to a few GHz, which is appropriate for applications in communication, remote sensing, RF linear accelerators, and power beaming.

One of the advantages of the scanning modulation over the conventional longitudinal modulation is seen when the beam voltage is high (~MeV). The advantage comes from the fact that the transverse mass of a relativistic electron is proportional to γm, while the longitudinal mass is proportional to $\gamma^3 m$. Here, γ is the electron energy relative to its rest mass. Scanning beam modulation is, therefore, easier by a factor of γ^2. Another advantageous feature of the above transverse klystron scheme is with the bending magnet. That is, the longitudinal effective mass of an electron gets negative in the magnet and consequently, the electron bunching is enhanced by the longitudinal self-field. This feature has previously been pointed out by Lau[6] in a different context. Along with these advantages the system is estimated to have high gain and efficiency without any help of extra passive cavities. The total system can be compact and simple. The next two sections provide an analytic estimation on how the bunching is accomplished in this system.

The transverse klystron concept described above does not have a guide magnetic field. Therefore, it is important to use a high energy electron beam to cancel out the transverse electrostatic field as much as possible. Even though the current is limited to a rather low value, the output power can be high since the electron energy and the efficiency are high. For a truly high power operation, however, we are pushed to a high current regime rather than a high voltage regime. A guiding magnetic field is essential in this regime, and various considerations are made in Sec. IV for this case. Finally, conclusions are made in Sec. V.

II. Single particle analysis

A schematic view of the device is shown in Fig. 1. A well collimated electron beam enters into the modulation cavity. There, the transverse momentum is modulated by the input signal, and through a ballistic drift, the beam gets displaced transversely by the time it reaches the bending magnet. The magnet modifies the transverse displacement into a longitudinal, and thus produces a longitudinal bunching of the electrons at the output cavity.

The z-axis indicated in Fig. 1 is the longitudinal coordinate axis along the unperturbed equilibrium beam orbit. Let us define a transverse coordinate r such that its unit vector $\hat{r}$ lies in the direction of modulation. In the bending magnet $\hat{r}$ is a radial unit vector and accordingly, the coordinate axis r rotates along the magnet. With another transverse coordinate y, in the direction going into the paper, (r, z, y) form right-handed local Cartesian (cylindrical) coordinates outside (inside) the magnet. The longitudinal coordinate z is related with the usual angular coordinate θ, by $z = r_0\theta$ inside the bending magnet. Here r_0 is the unperturbed orbit radius. Hence, the z coordinate of an arbitrary point is measured by the distance from the center of the modulation cavity to the projected point onto the z-axis in $\hat{r}$ direction. We denote the entry and the exit coordinates of the bending magnet with z_{in} and z_{out}, respectively. The drift distances between the modulation cavity and the magnet entry, and between the magnet exit and the output cavity are denoted with L_1 and L_2, respectively ($L_1 = z_{in}$).

Our primary concern for the rest of this paper is to estimate the longitudinal displacement δz of an electron with respect to the unperturbed electron departed at the same time, i.e.,

$$\delta z(t) = z(t) - z_0(t) \quad ,$$

where $z(t)$ is the actual electron position, $z_0(t) = v_{z0}(t - t_0)$, v_{z0} is the equilibrium beam velocity, and t_0 is the departure time at $z = 0$.

A. Modulation cavity

Let us imagine an electric field

$$E_r = E_0 \cos \omega t$$

in an input cavity, which modulates the transverse electron momentum. The field oscillates with a driving frequency ω. The modulated transverse velocity is given by

$$v_r = -\varepsilon_0 c \cos \omega t_0 \quad , \tag{1}$$

where c is the speed of light, t_0 is the time at which the electron is located at the center of the modulation cavity, and ε_0 is a small dimensionless parameter that measures the strength of the modulation;

$$\varepsilon_0 = 2eE_0\ell/\pi p_{z0} c \quad , \tag{2}$$

where ℓ is the cavity length, e is the absolute electron charge, and p_{z0} is the initial longitudinal momentum. Here we have assumed $\ell = \pi v_{z0}/\omega$ for a maximum deflection. A more realistic value of ε_0 can be given for a specific choice of mode.

For a TM_{210} mode in a rectangular cavity, as an example, the electric field is zero on axis and accordingly, the modulation is obtained by an oscillating magnetic field. Note that the longitudinal momentum is a dynamical constant, and the change in the longitudinal velocity is only through the change in the energy, $\delta\gamma$, which is in the second order in ε_0. Hence, the longitudinal displacement δz at $0 < z < z_{in}$ is proportional to ε_0^2, and can be neglected.

B. Initial conditions at the magnet entry

Through a ballistic drift from the modulation cavity, the electron obtains a transverse displacement at $z = z_{in}$

$$\delta r_{in} = -(\varepsilon_0 L_1/\beta_{z0}) \cos \omega t_0 \quad , \tag{3}$$

where $\beta_{z0} = v_{z0}/c$. Moreover,

$$\delta r' = -(\varepsilon_0/\beta_{z0}) \cos \omega t_0 \quad , \tag{4}$$

where the prime denotes a derivative with respect to z.

As Fig. 1 shows the bending magnet is assumed to have finite edge angles, ν_1 and ν_2. When the magnet edge is not normal to the equilibrium beam orbit, a modification must be taken for $\delta r'$. The change in δr is of the second order, and can be neglected. For simplicity in analysis we neglect any effect of the vertical fringe field, and assume that the vertical magnetic field, B_y, rises instantaneously at the edges. Intuitively, making the edge angle ν_1 positive is equivalent to superposing a normal magnet ($\nu_1 = 0$) with two triangular sector magnets of which the upper (lower) part has an opposite (same) polarity. It is clear that the incident parallel beam would get diverged. Hence, a positive angle ν_1 enhances the pitch angle $\delta r'$, and creates more path difference between the modulation and the output cavities so that the electron bunching is more efficient. Another advantageous role of the positive angle ν_1, as we will see below, is that the electrons are kicked in the vertical (y) direction to yield a focusing even without a finite field index.[7]

Let us now quantify these arguments. Figure 2 is a schematic picture near the magnet entrance. $\delta r'$ at point A is given by Eq. (4). The electron, however, enters into the magnet later at point B. Between the two points the electron trajectory is straight. The coordinate system, on the other hand, rotates following the curved longitudinal axis. The rotated angle at point B is $\delta\alpha = (\delta r_{in}/r_0)\tan\nu_1$ so that the *effective pitch angle is enhanced to*

$$\delta r'_{in} = -\left(1 + \frac{L_1}{r_0}\tan\nu_1\right)\frac{\varepsilon_0}{\beta_{z0}}\cos\omega t_0 \quad . \tag{5}$$

A further effect of the edge angle is observed in the vertical (y) direction. Let us denote the vertical displacement with δy, and its gradient with $\delta y'$. With a linear polarization of the modulation signal, as we are assuming in Sec. IIA, these are nonzero due to the finite beam emittance. With a circular modulation, they are the same as δr and $\delta r'$ except for a 90 degree phase difference. Assuming a stepwise rise of the vertical magnetic field at the entrance,

$$B_y = B_{0y}\theta(z - r\tan\nu_1) \quad ,$$

where $\theta(z)$ is a step function. This field alone, however, does not satisfy the Maxwell's equation, $div\ \vec{B} = curl\ \vec{B} = 0$, which is obvious because the field lines cannot be simply stopped at $z = r \tan \nu_1$. The accompaning radial field satisfies

$$\int dz B_r = -B_{0y} y \tan \nu_1 \quad .$$

This radial field gives electrons a vertical impulse, and changes the vertical velocity to

$$\delta y'_{in} = \delta y'(1 - \frac{L_1}{r_0} \tan \nu_1) \tag{6}$$

The positive edge angle, therefore, reduces the vertical pitch angle and gives rise to a beam focusing. A simple example of the focusing can be seen when we require $(L_1/r_0) \tan \nu_1 = 1$, i.e. $\delta y'_{in} = 0$. With an exit angle $\nu_2 = \nu_1$ and with a field index $n = 0$, it is obvious that the electrons will be focused at $L_2 = L_1$.

C. The bending magnet

We assume the fields of the bending magnet to be[8]

$$\begin{aligned} B_r &= -B_{0y} n \frac{z}{r_0} \quad , \\ B_y &= B_{0y}(1 - n\frac{r}{r_0}) \quad , \\ B_z &= B_{0z} \quad , \end{aligned}$$

where $n = -(r_0/B_{0y})[\partial B_y/\partial r]_{r=0}$ is the field index, and the guide field B_{0z} is zero in the present section. The equilibrium orbit is defined by

$$r_0 = \frac{v_{z0}\gamma_0}{\Omega_{0y}} \quad ,$$

$$
\begin{aligned}
\gamma_0 &= \left(1 - \beta_{z0}^2\right)^{-1/2} = \left(1 + \Omega_{0y}^2 r_0^2 / c^2\right)^{1/2} \quad , \\
z_0(t) &= \frac{\Omega_{0y} r_0}{\gamma_0}(t - t_{in}) \quad ,
\end{aligned}
$$

where $\Omega_{0y} = eB_{0y}/mc$ is the nonrelativistic electron cyclotron frequency.

Assuming dynamical quantities have small perturbations from the equilibrium values, i.e. $\gamma = \gamma_0 + \delta\gamma$, $r = \delta r$, $y = \delta y$, and $z = z_0 + \delta z$, we substitute these quantities into the equation of motion and linearize with respect to the small perturbations. The resulting equations of motion are

$$
\delta r'' + k_r^2 \delta r = k_z \delta y' + \frac{1}{r_0 \beta_{z0}^2} \frac{\delta\gamma}{\gamma_0} \quad , \tag{7}
$$

$$
\delta y'' + k_y^2 \delta y = -k_z \delta r' \quad , \tag{8}
$$

$$
\delta z' + \frac{\delta r}{r_0} = \frac{\delta v_{z,in}}{v_{z0}} \quad , \tag{9}
$$

where $k_r = (1-n)^{1/2}/r_0$, $k_y = n^{1/2}/r_0$, $k_z = B_{0z}/(r_0 B_{0y})$, and $\delta v_{z,in} = \delta v_z(z = \ _{in})$ is a constant. For the present section, assuming a zero electron temperature, $\delta\gamma$ and $\delta v_{z,in}$ are proportional to ε_0^2, and is neglected. Moreover, $k_z = 0$ without the guide field. Equations (7) - (9) are readily solved with the initial conditions (3), (5), and (6) to give

$$
\begin{aligned}
\delta r(z) &= -\frac{\varepsilon_0}{\beta_{z0} k_r} \cos \omega t_0 \\
&\quad \cdot \left[\left(1 + \frac{L_1}{r_0} \tan \nu_1\right) \sin k_r (z - z_{in}) + L_1 k_r \cos k_r (z - z_{in})\right] \quad . \qquad (10) \\
\delta y(z) &= \frac{\delta y_{in}}{L_1 k_y} \left[\left(1 - \frac{L_1}{r_0} \tan \nu_1\right) \sin k_y (z - z_{in}) + k_y L_1 \cos k_y (z - z_{in})\right] \qquad (11) \\
\delta z(z) &= (1-n)^{-1/2} \frac{\varepsilon_0}{\beta_{z0} k_r} \cos \omega t_0
\end{aligned}
$$

$$\cdot \left[\left(1 + \frac{L_1}{r_0} \tan \nu_1\right) (1 - \cos k_r(z - z_{in})) + L_1 k_r \sin k_r(z - z_{in}) \right] \quad (12)$$

At the end of the magnet $k_r(z - z_{in}) = (1 - n)^{1/2}\alpha$, where α is the subtended angle of z-axis in the bending magnet over the radius r_0.

D. Focusing conditions

Since the electron beam has been modulated transversely, refocusing of the beam at the position of output cavity is important. Furthermore, focusing in y-direction is also preferred to overcome the beam spread due to the finite emittance. The bending magnet with positive edge angles provides the required focusing. The focusing requirements in both directions are

$$\begin{aligned} (A) \quad \delta r_{out} &= -L_2 \delta r'_{out} \; , \\ (B) \quad \delta y_{out} &= -L_2 \delta y'_{out} \; , \end{aligned}$$

where quantities with the subscript "out" stand for the values immediately after the magnet exit.

Using the solution given by Eq. (10) we can express each side of the condition (A) as

$$\begin{aligned} \delta r_{out} &= -\frac{\varepsilon_0}{\beta_{z0} k_r} \cos \omega t_0 \left(1 + \frac{L_1}{r_0} \tan \nu_1\right) \sqrt{1 + \xi_1^2} \sin \left[(1 - n)^{1/2}\alpha + \phi_1\right] \\ \delta r'_{out} &= -\frac{\varepsilon_0}{\beta_{z0}} \cos \omega t_0 \left(1 + \frac{L_1}{r_0} \tan \nu_1\right) \sqrt{1 + \xi_1^2} \cos \left[(1 - n)^{1/2}\alpha + \phi_1\right] \\ &\quad \cdot \left(1 + \frac{L_2}{r_0} \tan \nu_2\right)^{-1} \end{aligned}$$

where $\xi_1 = (1-n)^{1/2} L_1/(r_0 + L_1 \tan\nu_1)$ and $\phi_1 = \tan^{-1}\xi_1$. Here, the extra factor involving $\tan\nu_2$ has been multiplied to account for the effect of the edge angle ν_2 at the magnet exit by the same reason as at the magnet entrance. Substituting these into the condition (A) we find a focusing condition in the r-direction,

$$(1-n)^{1/2}\alpha = l\pi - \phi_1 - \phi_2 \quad , \tag{13}$$

where l is an integer preferably 1 in the experiment, $\phi_2 = \tan^{-1}\xi_2$, and $\xi_2 = (1-n)^{1/2} L_2/(r_0 + L_2 \tan\nu_2)$. Similarly, using Eq. (12), we translate the condition (B) into

$$n^{1/2}\alpha = m\pi - \psi_1 - \psi_2 \quad , \tag{14}$$

where m is an integer preferrably either 0 or 1, $\psi_i = \tan^{-1}\eta_i$ $(i = 1,2)$, and $\eta_i = n^{1/2} L_i/(r_0 - L_i \tan\nu_1)$.

Now imposing the condition (13) to Eq. (12), the longitudinal displacement δz at the magnet exit, and thus at the output cavity, is given by

$$\delta z_{out} = \frac{\varepsilon_0}{\beta_{z0}(1-n)}(r_0 + L_1 \tan\nu_1)\left[1 + \left(\frac{1+\xi_1^2}{1+\xi_2^2}\right)^{\frac{1}{2}}\right]\cos\omega t_0 \tag{15}$$

Equation (15) suggests that for a given value of ξ_1 the optimum displacement is obtained when $\xi_2 = 0$, or equivalently, $L_2 = 0$. The configuration with no second drift region has still another advantage that the electron bunching, which has been obtained in the bending magnet, is not deteriorated by the effect of a longitudinal self-field. A positive field index also enhances the displacement. The focusing condition (13), however, shows that a large value of α is necessary when $\xi_2 = 0$ or $n \approx 1$.

E. Electron density

Let us imagine a string of particles distributed uniformly at an initial time. Let z_{0j} be the initial location of the j-th particle. The electron distribution after the bending magnet is determined by displacements δz_j of the individual particles;

$$\delta z_j = \mu_0 \cos k z_{0j} \quad ,$$

where $k = \omega / v_{z0}$, and μ_0 is the coefficient of $\cos \omega t_0$ in Eq. (15). We can express the line density of the electron distribution at a given instantaneous time with

$$n(z) = \sum_j \delta(z - z_{0j} - \delta z_j) \quad , \tag{16}$$

where $\delta(z)$ is the Dirac delta function, and the summation is over all electrons. Fourier-analysing the density $n(z)$,

$$n(z) = \int_{-\infty}^{\infty} dp\, e^{ipz} \rho_p \quad , \tag{17}$$

we find

$$\rho_p = n_0 \sum_{m=-\infty}^{\infty} (-i)^m J_m(p\mu_0) \delta(p + mk) \quad , \tag{18}$$

where n_0 is the equilibrium line density, and J_m is the m-th order Bessel function of the first kind. Substituting Eq. (18) back into Eq. (17) we obtain the electron line density

$$n(z) = n_0 \left[1 + 2 \sum_{m=1}^{\infty} J_m(mk\mu_0) \sin mkz \right] \quad . \tag{19}$$

Considering just the fundamental harmonic, the amplitude, $2n_0 J_1(k\mu_0)$, obtains its maximum value $1.16 n_0$ at $k\mu_0 = 1.841$. In case $k\mu_0 < 1$, we can approximate the density modulation in the fundamental harmonic

$$\delta n(z) \simeq n_0 k \mu_0 \sin kz \quad . \tag{20}$$

Density modulation becomes difficult on low frequencies. In the conventional two-cavity klystron the electron bunching is given with $\mu_0 = L\varepsilon_0/(\beta_{z0}\gamma^2)$, where L is the drift length. For a relativistic electron beam, say $\gamma > 2$, therefore, the bending magnet with a transverse modulation can easily achieve an order of magnitude higher modulated density for the same modulation strength (ε_0) and a comparable device size. Furthermore, when we increase the current, the electron bunching is deteriorated by the self-field in the conventional klystron, while the self-field enhances the bunching in the present scheme, as we will see in the next section.

III. Some collective effects

A. Effect of the longitudinal self-field

We assume that the electron beam is cold. As we saw in Sec. II the logitudinal displacement δz is developed on drifting through the bending magnet. Let us denote

$$\delta z(z) = \mu(z) \cos \omega t_0 \quad , \tag{21}$$

where $\mu(z)$ is the amplitude of the displacement, having bounary values $\mu(z_{in}) = 0$, and $\mu(z_{out}) = \mu_0$. Here, ωt_0 is a convective constant attached to each particle, and an equivalent expression in the space-time coordinate is $\omega t - kz$ with $k = \omega / v_{z0}$. A collection of particles with δz as in Eq. (21) form a density perturbation in the fundamental harmonic

$$\frac{\delta n}{n_0} = k\mu(z) \sin(\omega t - kz) \quad , \tag{22}$$

where $k\mu(z) < 1$ is assumed. In the limit of $kr_b \ll 1$, where r_b is the electron beam radius, the density of Eq. (22) produces a longitudinal electric field

$$E_z = gn_0 ek^2 \mu(z) \cos(\omega t - kz) = gn_0 ek^2 \delta z(z) \quad , \tag{23}$$

where $g = (1 + \ln(a/r_b))/\gamma_0^2$, and a is the radius of a perfectly conducting wall. Using this field for the longitudinal equation of motion, and rearranging Eq. (7) for the radial, we arrive at a set of coupled equations;

$$\delta r'' - \kappa_1^2 \delta r = \kappa_2 \delta z' \quad , \tag{24}$$

$$\delta z'' + k_s^2 \delta z = -\frac{\delta r'}{r_0} \quad , \tag{25}$$

where $k_s^2 = gk^2 n_0 e^2/(m\gamma_0^3 v_{z0}^2)$, $\kappa_1^2 = (\gamma_0^2 - (1-n))/r_0^2$, $\kappa_2 = \gamma_0^2/r_0$, and use has been made of $\delta\gamma = \gamma_0^3 v_{z0}\delta v_z/c^2$ and $\delta v_z/v_{z0} = \delta z' + \delta r/r_0$ for Eq. (24).

An intuitive understanding of the implication of the two equations can be made by neglecting the $\delta r''$ term. We immediately find that the coefficient of $\delta z''$ in Eq. (25) can be negative, implying an effective negative mass[6,9] for the longitudinal motion. For $n = 0$, the effective mass is $m_{eff} = -(\gamma_0/\beta_{z0}^2)m$. The negative mass will result in an exponential growth of the displacement.

Equations (24) and (25) are decoupled in the limit $r_0 \to \infty$. This limit represents the free space drift, showing a longitudinal plasma oscillation with a wavelength $2\pi/k_s$. This oscillation sets an upper bound for the drift length between the magnet exit and the output cavity. $k_s L_2 \ll 1$ is required not to deteriorate the modulated density achieved in the bending magnet.

Equations (24) and (25) are solved easily, though a little algebra is needed. Along with the initial conditions $\delta z = 0$, $\delta z' = -\delta r_{in}/r_0$, $\delta r = \delta r_{in}$, and $\delta r' = \delta r'_{in}$, where δr_{in} and $\delta r'_{in}$ are as in Eqs. (3) and (5), the solutions are

$$\begin{aligned}
\delta r(z) &= \delta r_{in}\frac{p_+^2 + k_r^2}{p^2}\cos p_-(z - z_{in}) - \delta r'_{in}\frac{p_-(p_+^2 - \kappa_1^2)}{\kappa_1^2 p^2}\sin p_-(z - z_{in}) \\
&\quad + \delta r_{in}\frac{p_-^2 - k_r^2}{p^2}\cosh p_+(z - z_{in}) + \delta r'_{in}\frac{p_+(p_-^2 + \kappa_1^2)}{\kappa_1^2 p^2}\sinh p_+(z - z_{in}) \qquad (26) \\
\delta z(z) &= -\frac{\delta r_{in}}{r_0 p^2}\left(p_- \sin p_-(z - z_{in}) + p_+ \sinh p_+(z - z_{in})\right) \\
&\quad - \frac{\delta r'_{in}}{r_0 p^2}\left(\cosh p_+(z - z_{in}) - \cos p_-(z - z_{in})\right) \quad , \qquad (27)
\end{aligned}$$

where $p_\pm = (1/\sqrt{2})[p^2 \mp (k_r^2 + k_s^2)]^{1/2}$, and $p^2 = [(k_r^2 + k_s^2)^2 + 4k_s^2\kappa_1^2]^{1/2}$.

These solutions have an exponential dependence in z with the e-folding rate of p_+. p_+ is zero for $k_s = 0$, and in this case the solutions reduce to the former solution in Sec. II (Eqs. (10) and (12)). When k_s is comparable to k_r, $p_+ r_0$ is of order unity, and hence, a significant enhancement of electron bunching is observed. Since k_s is proportional to $(\gamma_0\beta_{0z})^{-5/2}$ for given frequency and current, the effect is large especially for low electron energy. It is noticed that the positive field index increases p_+. The oscillation wavenumber p_- also increases by the space charge effect, and this brings the focal point closer to the magnet.

B. Effect of the energy spread

Let us imagine an electron whose energy is $\gamma = \gamma_0 + \delta\gamma$. Here $\gamma_0 = (1 + (r_0\Omega_0/c)^2)^{1/2}$ is the equilibrium beam energy. The energy mismatch $\delta\gamma$ may be caused by the beam temperature and/or by the voltage ripple at the electron gun. We neglect, however, the energy variation due to the input modulation and to the self-field, so that the energy may be treated as a dynamical constant. An effect of the finite emittance angle is also neglected since it is assumed to be much less than ε_0. We estimate the influence of $\delta\gamma$ on δz.

In the free drift regions outside the bending magnet δz is produced by the longitudinal velocity difference, $v_z - v_{z0}$;

$$\delta z_{\gamma,1} = \frac{L_1 + L_2}{\gamma_0^2 - 1} \cdot \frac{\delta\gamma}{\gamma_0} \tag{28}$$

In the bending magnet, we already have the governing equations (Eqs. (7) and (9)). Here, care must be given to the integration constant $\delta v_{z,in}$ since it is related to $\delta\gamma$; $\delta v_{z,in} = (\delta\gamma/\gamma_0)(v_{z0}/(\gamma_0^2 - 1))$. Solving the radial equation first, using the initial conditions δr_{in} and $\delta r'_{in}$ as in Sec. II, and substituting the solution into the longitudinal equation, the total electron displacement is found as follows.

$$\delta z = \delta z_{\epsilon_0} + \delta z_{\gamma,2} \quad ,$$

where

$$\delta z_{\gamma,2} = \frac{\delta\gamma}{\gamma_0\beta_{z0}^2}\left[\left(\frac{1}{\gamma_0^2} - \frac{1}{1-n}\right) r_0\alpha + \frac{r_0}{(1-n)^{3/2}}\sin(1-n)^{1/2}\alpha\right] \quad , \tag{29}$$

and δz_{ϵ_0} is the displacement in a monoenergetic beam estimated previously (Eq. (15)). Adding the contributions of Eqs. (28) and (29) the total displacement due to $\delta\gamma$ is given ;

$$\delta z_\gamma = \frac{\delta\gamma}{\gamma_0\beta_{z0}^2}\left[\frac{L}{\gamma_0^2} + \frac{r_0}{(1-n)^{3/2}}\sin(1-n)^{1/2}\alpha - \frac{r_0\alpha}{1-n}\right] \quad , \tag{30}$$

where $L = L_1 + L_2 + r_0\alpha$ is the total equlibrium path length. Notice that δz_γ vanishes when the quantity in the square bracket is zero. The effect of energy spread on the longitudinal bunching, therefore, can be taken away, even though the spread deteriorates transverse focusing. If $\delta\gamma$ is due to the electron temperature, or more exactly, if the equilibrium kinetic distribution function is independent of time, the additional displacement in (30) results in a degradation of density modulation which is estimated to be

$$\frac{n(z)}{n_0} = 1 + 2\sum_{m=1}^{\infty}\exp\left(-\frac{1}{2}m^2k^2\sigma^2\right) J_m(mk\mu_0)\sin mkz \quad ,$$

where $\sigma = \sqrt{<\delta z_\gamma^2>}$.

IV. Guiding magnetic field

In previous sections we have considered a transverse klystron without the guiding magnetic field. In the configuration, we have implicitly assumed that the electron energy is sufficiently high for a given electron current so that the electrostatic defocusing effect may be neglected. A moderately high output power can be expected even with a relatively low current since the electron energy is high. The paraxial beam envelope equation[10] shows that the electrostatic defocusing is determined by the relativistic perveance $I/\gamma^3\beta^3$. The perveance must be kept as small as possible in order to achieve a high efficiency. This is because any spread in δr_{in} and $\delta r'_{in}$ will result in the spread in δz_{out}, and thus in deterioration of density modulation. It is expected, therefore, that the output power will be saturated at certain limiting current. Obviously, the limiting current increases with the electron energy.

Beyond the limiting current, stable transport of the electron beam ultimately requires a guiding magnetic field. The guide field, however, wipes out the scanning beam modulation. The residual $E \times B$ drift of the guiding center is usually small unless the input power for modulation is extremely large. As we will see in Sec. IVA the electron bunching is rather inefficient if we rely on the small guiding center shift. A slow adiabatic contouring of the guide field between the modulation cavity and the bending magnet has been considered by Mako and Godlove[4] in order to enhance the guiding center shift. Here, various other options are considered.

A. Beam centroid orbit inside the bending magnet

Let us consider a solid pencil beam injected into the bending magnet. The electrostatic force is not negligible in the presently interested high perveance regime. At the beam centroid, however, the electrostatic forces cancel by symmetry, and the equation of motion is identical to the single particle orbit. Hence, the governing equations are already given in Sec. II (Eqs. (7)-(10)). For simplicity, we choose a field index $n = 0.5$. The solution, however, turns out to be insensitive to this choice.

Equations (7) and (8) can be combined into a complex form to give the transverse trajectory

$$\begin{aligned}\delta R &= \delta r + i\delta y \\ &= \frac{\gamma_0^2}{r_0 k_r^2}\frac{\delta v_{z,in}}{v_{z0}} + \frac{1}{k_+ + k_-}\left(k_+\delta R_{in} - i\delta R'_{in} - k_+\frac{\gamma_0^2}{r_0 k_r^2}\frac{\delta v_{z,in}}{v_{z0}}\right)e^{ik_-(z-z_{in})} \\ &\quad + \frac{1}{k_+ + k_-}\left(k_-\delta R_{in} + i\delta R'_{in} - k_-\frac{\gamma_0^2}{r_0 k_r^2}\frac{\delta v_{z,in}}{v_{z0}}\right)e^{ik_+(z-z_{in})} \quad , \quad (31)\end{aligned}$$

where $k_\pm = (\sqrt{k_z^2 + 4k_r^2} \pm k_z)/2$, and δR_{in} and $\delta R'_{in}$ are unspecified initial conditions at $z = z_{in}$ in complex forms similar to δR. Here, use has been made of $\delta\gamma = \gamma_0^3\beta_{z0}\delta\beta_{z,in}$. It is noted that k_r differs from k_z by two orders of magnitude, for a guide field of an order of a kilogaus, and for the equilibrium orbit radius of a few tens of centimeters. Hence, $k_+ \approx k_z \gg k_- \approx (k_r/k_z)k_r$.

The longitudinal displacement δz is obtained by Eq. (9) using δr given by the real part of Eq. (31).

$$\delta z = \left(1 - \frac{\gamma_0^2}{1-n}\right)\frac{\delta v_{z,in}}{v_{z0}}(z - z_{in})$$

$$
-\frac{1}{r_0 k_z k_-}\left[k_+\delta r_{in} + \delta y'_{in} - k_+ r_0 \frac{\gamma_0^2}{1-n}\frac{\delta v_{z,in}}{v_{z0}}\right]\sin k_-(z - z_{in})
$$

$$
-\frac{1}{r_0 k_z k_-}[k_+\delta y_{in} - \delta r'_{in}](1 - \cos k_-(z - z_{in})) \quad . \tag{32}
$$

Here, we have dropped the fast oscillating terms since they have a negligible contribution after integration. Now we wish to express (32) in terms of the guiding center coordinates. A little geometrical exercise shows that the guiding center $R_c = (r_c, y_c)$ at the magnet entrance is given by

$$
R_{c,in} = \left(\delta r_{in} + \frac{\delta y'_{in}}{k_z} \quad , \quad \delta y_{in} - \frac{\delta r'_{in}}{k_z} \right) \quad .
$$

Substituting this, and neglecting small terms proportional to k_r/k_z, we have the intuitive result

$$
\delta z_{out} = \frac{\delta v_{z,in}}{v_{z0}} r_0 \alpha - r_{c,in} \quad \alpha \, , \tag{33}
$$

where $\alpha = (z_{out} - z_{in})/r_0$. Here, the first term is the displacement due to longitudinal velocity variation, as in the conventional klystron, and the second term is due to the path difference along the circular guiding center orbit. All other details of the initial conditions are wiped out because of the strong guide field. Hence, our effort in subsequent sections will be focused to finding the ways of modulating the two quantities, v_z and r_c.

Since we are interested in a high current beam, we should be more concerned with the effect of self-field. The transverse electrostatic field is not a worry since we have a strong guide field. The longitudinal self-field is our concern. Its effect is contained in the scaling parameter k_s as we saw in Sec. III. In previous sections the the longitudinal self-field was a merit. The effective negative mass actually helps the electron bunching. In the presence of a guide field, however, the negative mass instability is turned off. This can be understood when we imagine how the effective mass of an electron becomes negative. When the electron is forced in one azimuthal direction the electron is accelerated in that direction and the Larmor radius changes. And then, this radius change, in turn, results in an azimuthal acceleration in reverse direction to the force. Hence, to have a negative mass, the radius change is essential, which is prevented in the presence of a guide field. To see this more explicitly we observe the equation of motion including the space charge effect. Starting from Eqs. (7), (8) and (25) we average the equations over fast time scale defined by a strong guide field. Then the equations reduce to those for the guiding center r_c and average longitudinal displacement z_c ;

$$r_c''(z) - \left(\frac{k_y}{k_z}\right)^2 \kappa_1^2 r_c(z) = \left(\frac{k_y}{k_z}\right)^2 \kappa_2 \delta z_c'(z) \ , \tag{34}$$

$$z_c''(z) + k_s^2 z_c(z) = -\frac{r_c'(z)}{r_0} \ . \tag{35}$$

The solution to these two equations contains parameters $p_\pm$ which are similar to the ones in Sec. III.

$$p_\pm = \frac{1}{\sqrt{2}}\left[p^2 \mp \left(k_s^2 + \left(\frac{k_y}{k_z}\right)^2 k_r^2\right)\right]^{1/2} \tag{36}$$

$$p^2 = \left[\left(k_s^2 + \left(\frac{k_y}{k_z}\right)^2 k_r^2\right)^{1/2} + 4\left(\frac{k_y}{k_z}\right)^2 \kappa_1^2 k_s^2\right]^{1/2} \tag{37}$$

Since $k_y/k_z \sim O(10^{-2})$, $k_y \sim 10^{-1}$ cm^{-1} and typically, $k_s > 10^{-2}$ cm^{-1}, k_s^2 is the most dominant quantity in (36) and (37). Hence,

$$
\begin{aligned}
p_+ &\approx \frac{k_y}{k_z}\kappa_1 \ , \\
p_- &\approx k_s \ ,
\end{aligned}
$$

and the solution is approximated to

$$
z_c(z) \approx \frac{1}{k_s}\left(\frac{r_{c,in}}{r_0} + \frac{\delta v_{z,in}}{v_{z0}}\right)\sin k_s(z - z_{in}) \ . \tag{38}
$$

Notice that the negative mass effect has been turned off with its tiny growth rate p_+. The solution (38) reduces to the former solution (33) without considering the space charge effect when $k_s(z - z_{in}) \ll 1$. The former grows indefinitely, while the latter saturates at $k_s L = \pi/2$, and then decays. Here L is the total drift length. This is merely due to the free space plasma oscillation. As a numerical example, if $I = 100$ A, $\gamma = 2$, and $\omega = 10^{10}$ sec^{-1}, then k_s is approximately 10^{-2} cm^{-1}, and the saturation occurs at $L = 1.5$ m. If we either increase the current to a kiloampere or decrease the energy to $\gamma = 1.48$, however, the saturation length reduces to 15 cm.

B. Resonant modulation

Let us first consider a situation where the whole system, from the electron gun to the output cavity, is immersed in a guide field. High perveance electron beams would prefer this situation. The disadvantage is, as mentioned previously, that the (transverse) beam modulation is difficult. Field contouring or multiple passive cavities may be employed to enhance the modulation. As an alternative option we consider here a resonant modulation, i.e., matching the cyclotron frequency to the modulation frequency. The system can be more compact (no drift region) and be relatively simple. To estimate how much magnetic field is required and how much beam current is allowed with the resonance condition we consider the simple solid beam stability requirement ;

$$\frac{2\omega_p^2}{\gamma^2\omega_z^2} < 1 \quad ,$$

where ω_p and ω_z are relativistic plasma and cyclotron frequencies, respectively. For $\gamma = 2$ and $\omega = \omega_z \sim 10^{11}$ sec^{-1} (16 GHz), the required guide field B_0 is 11.4 kG, and the limiting current density J_c is ~ 52 kA/cm^2. On the other hand, for $\gamma = 2$ and $\omega = 10^{10}$ sec^{-1} (1.6 GHz), $B_0 = 1.1$ kG, and $J_c \sim 0.5$ kA/cm^2. These numerical values show practical applicability of the resonant modulation at frequencies of a few GHz.

Now let us consider the beam centroid motion in the modulation cavity;

$$\begin{aligned} \ddot{r} &= \omega_z \dot{y} \quad , \\ \ddot{y} &= -\omega_z \dot{r} - \frac{eE_0}{m\gamma_0}\cos\omega t_0 \quad , \end{aligned}$$

where $\omega_z = eB_{0z}/\gamma_0 mc$, the overdots denote time derivatives, and the coordinate system is identical as before except that the $z = 0$ point is now chosen at the entrance of the input cavity rather than at the center. Let us also denote the initial time t_0 to be the time at which the particle enters into the cavity. Equating $\omega_z = \omega$, and using initial conditions $r(t_0) = \dot{r}(t_0) = y(t_0) = \dot{y}(t_0) = 0$, the solution shows that the guiding center $R_c = (r_c, y_c) = (r + \dot{y}/\omega, y - \dot{r}/\omega)$ at time t is

$$R_c = \left(\frac{2\epsilon_1 c}{\omega}[\sin\omega t_0 - \sin\omega t] \ , \ 0 \right) \quad ,$$

where $\varepsilon_1 = eV_0/2h\pi p_z c$ is the normalized input signal strength. Here $V_0 = E_0\ell$, ℓ is the cavity length, and $h\pi = \omega\Delta t$ is the total phase change of input signal during the transit time Δt. Comparing to the previous normalization, $\varepsilon_1 = \varepsilon_0/4$ for $h = 1$. It is noticed that the resonance has no effect on the location of the guiding center. At times $\omega(t - t_0) = (2n + 1)\pi$ (n = integer), the guiding center shifts maximally, and it can be shown that the beam centroid orbit satisfies

$$\left[r - \frac{4\varepsilon_1 c}{\omega}\sin\omega t_0\right]^2 + y^2 = \left[(2n + 1)\pi\frac{\varepsilon_1 c}{\omega}\right]^2$$

Hence, the Larmor radius grows linearly in time.

Even though the resonant modulation does not enhance the guiding center shift directly, the growth in Larmor radius gives us indirect ways of enhancing it. Note again that the radial location of the guiding center is given by $r_c = r + \dot{y}/\omega_z$. Here r_c oscillates with a small amplitude $4\varepsilon_1 c/\omega$ because the growing dependences of r and $\dot{y}$ cancel each other. By breaking the cancellation, therefore, we can restore the linear growth. To do so, we may have, for example,

(i) an instantaneous kick in the y direction,

(ii) an instantaneous raise of the guide field.

We have already seen an example of (i) at the magnet entrance with a finite edge angle. In this case a radial fringe field kicks the beam in the y direction. Assuming the magnet entrance is located at the end of the modulation cavity, the guiding center shift is estimated to be

$$r_c = \frac{\varepsilon_1 c}{\omega}\left[4 - \frac{v_z}{r_0\omega}(2n + 1)\pi\tan\nu_1\right]\sin\omega t_0 \quad .$$

Hence, a negative edge angle is required to enhance the shift. The enhancement is not efficient since $v_z/(r_0\omega)$ is small for a frequency above a GHz. This suggests that the fringe field is too weak. An external radial field, therefore, might be more useful.

A stepwise rise of the guide field changes the Larmor radius. Conservation of canonical momentum, $P_\theta = \gamma m v_\theta r - (er/c)A_\theta$, estimates

$$\frac{R_{L1}}{R_{L0}} = \frac{1 + (B_{z0}/B_{z1})}{2} \quad , \tag{39}$$

where R_{L1} (R_{L0}) is the Larmor radius in the field strength B_{z1} (B_{z0}). Hence, we can convert 25 % of the Larmor radius into guiding center shift with a raise of $B_0 \rightarrow 2B_0$. Care must be given here to the longitudinal motion since a magnetic cusp introduces an additional kick in the longitudinal direction. This kick introduces modulation of v_z in the second harmonic.

C. Modulation outside of the guide field

Even though high perveance beams prefer the whole system immersed in a guide field, ease of scanning modulation without a guide field forces us to consider configurations in which the modulation cavity is located out of the guide field. The guide field is assumed to have a half cusp structure, i.e. $B_z = 0(B_{0z})$ at $z < z_{in}$ ($z > z_{in}$). In such a configuration a focusing lens may be placed right after the electron gun so that the beam waist is located down at the position of the cusp. On entering into the half cusp, part of the longitudinal energy is transferred to the transverse energy so that the electrons gyrate around the field lines. The Larmor radius is

$R_L = \delta r_{in}/2$, where δr_{in} is the radial displacement at the cusp with respect to the symmetry axis of guiding field lines. Hence, we have a guiding center $r_c = \delta r_{in}/2$, which oscillates with a $\cos \omega t_0$ dependence. As described in Sec. IVA this oscillating guiding center can be transformed into an electron bunching when a bending magnet is placed on top of the guide field. The electron bunching, however, can be achieved even without the bending magnet since some of the longitudinal energy has been transferred to the transverse energy, and as a result, the longitudinal velocity has been modulated. Since the energy is conserved across the cusp, the velocity modulation is estimated to be

$$\delta v_z \approx -\frac{\omega_z^2}{8 v_{z0}} \delta r_{in}^2 \quad .$$

With a $\cos \omega t_0$ dependence in δr_{in}, therefore, δv_z results in an electron density modulation at the second harmonic to the modulation frequency.

V. Conclusions

Scanning beam modulation has recently been brought into great attention as a new technique for generation of high power coherent radiation with high efficiency. The transverse klystron scheme investigated in this paper utilizes the ease of scanning modulation at a relativistic beam energy. The system can be operated with high efficiency and gain without any auxiliary passive cavities. As a result, the total system can be simple and compact. In this paper we have obtained an analytic solution to the scheme. Characteristics of the electron density modulation on various design parameters are clarified. Focusing properties of the bending magnet, the effect of energy spread, and the effect of longitudinal self-field have also been considered. It is noted that the density modulation is enhanced by the self-field through an effective negative mass, and that there exists a condition that gets rid of the effect of energy spread.

Efficient operation of the transverse klystron without the guide field strictly requires a high brightness and a low perveance of the electron beam. To relax the requirement on low perveance, we consider employing a guide magnetic field. With the guide field the electron density modulation is obtained through a guiding center shift and a longitudinal velocity modulation. The longitudinal velocity modulation is obtained when the electrons cross a discontinuous guide field. As possible methods for overcoming the difficulty in scanning modulation in the presence of guide fields, a resonant modulation and a configuration with a half cusp field have been investigated. The resonant modulation requires an additional procedure which converts the resonant Larmor orbit into guiding center shifts. The half cusp field can be employed either with or without the bending magnet to produce a desired density modulation.

Acknowledgement

The authors thank Dr. F. Mako and Dr. T. Godlove for many helpful discussions. This work has been supported by the Office of Naval Research.

References

[1] M. M. Karliner, E. V. Kozyrev, I. G. Makarov, O. A. Nezhevenko, G. N. Ostreiko, B. Z. Persov, and G. V. Serdobintsev, *Nucl. Inst. Meth.*, A269, 459 (1988)

[2] W. M. Manheimer, *IEEE Tran. Plas. Sci.*, PS-18, No. 3, 632 (1990)

[3] K. R. Chu and J. L. Hirshfield, *Phys. of Fluids*, 21, 461 (1978)

[4] F. Mako and T. F. Godlove, private communication

[5] G. Faillon, *IEEE Trans. Nucl. Sci*, NS-32, No. 5, 2945 (1985)

[6] Y. Y. Lau, *Phys. Rev. Lett.*, 53, 395 (1984)

[7] H. A. Enge, in "Focusing of Charged Particles", Vol II, (Academic Press, New York), Edited by A. Septier (1967)

[8] P. Sprangle and C. A. Kapetanakos, *J. Appl. Phys.*, 49, 1 (1978)

[9] R. W. Landau and V. K. Neil, *Phys. of Fluids*, 9, 2412 (1966)

[10] M. Reiser, *IEEE Trans. Nucl. Sci.*, NS-32, No. 5, 2201 (1985)

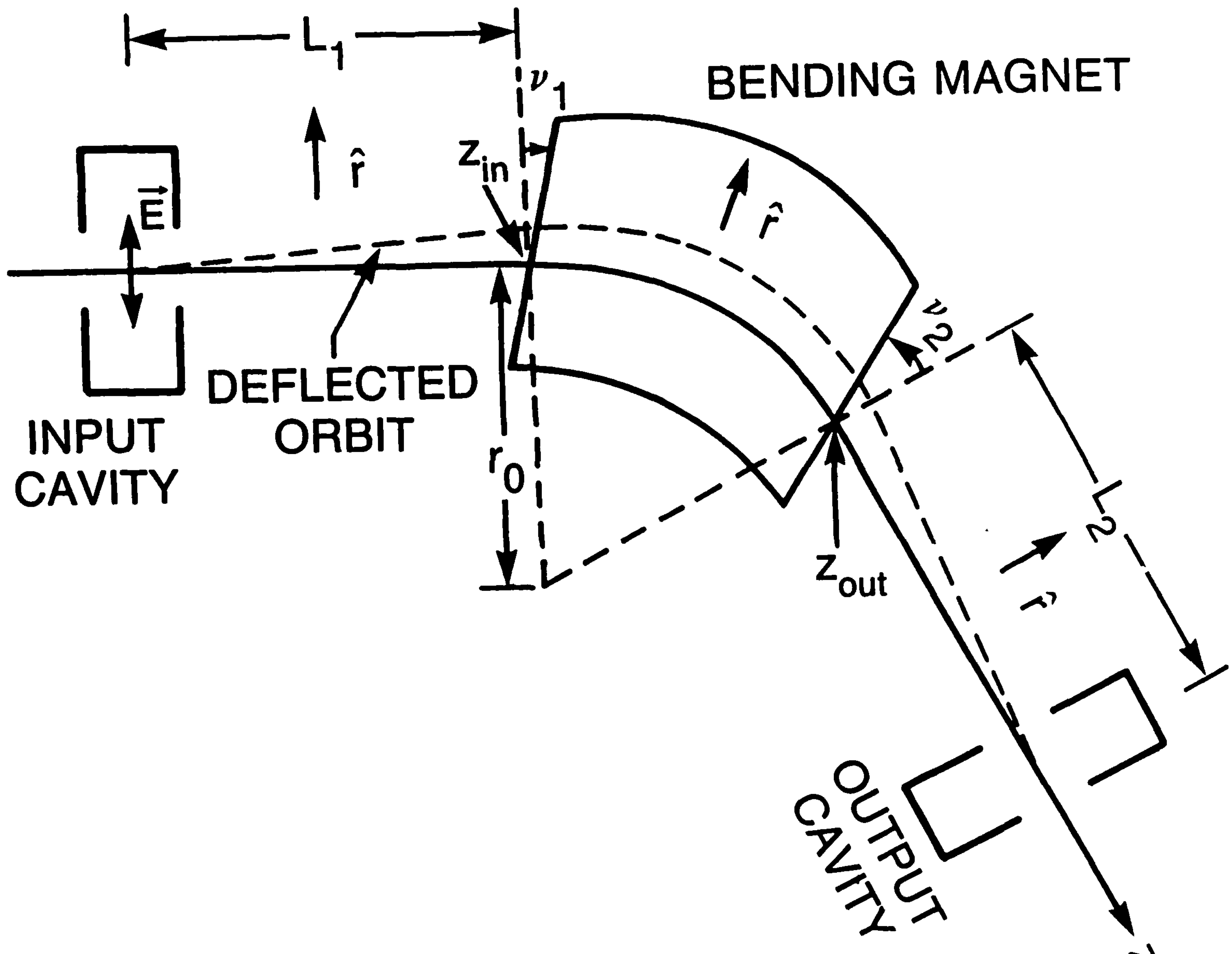

Fig. 1 — Schematic configuration of the transverse klystron

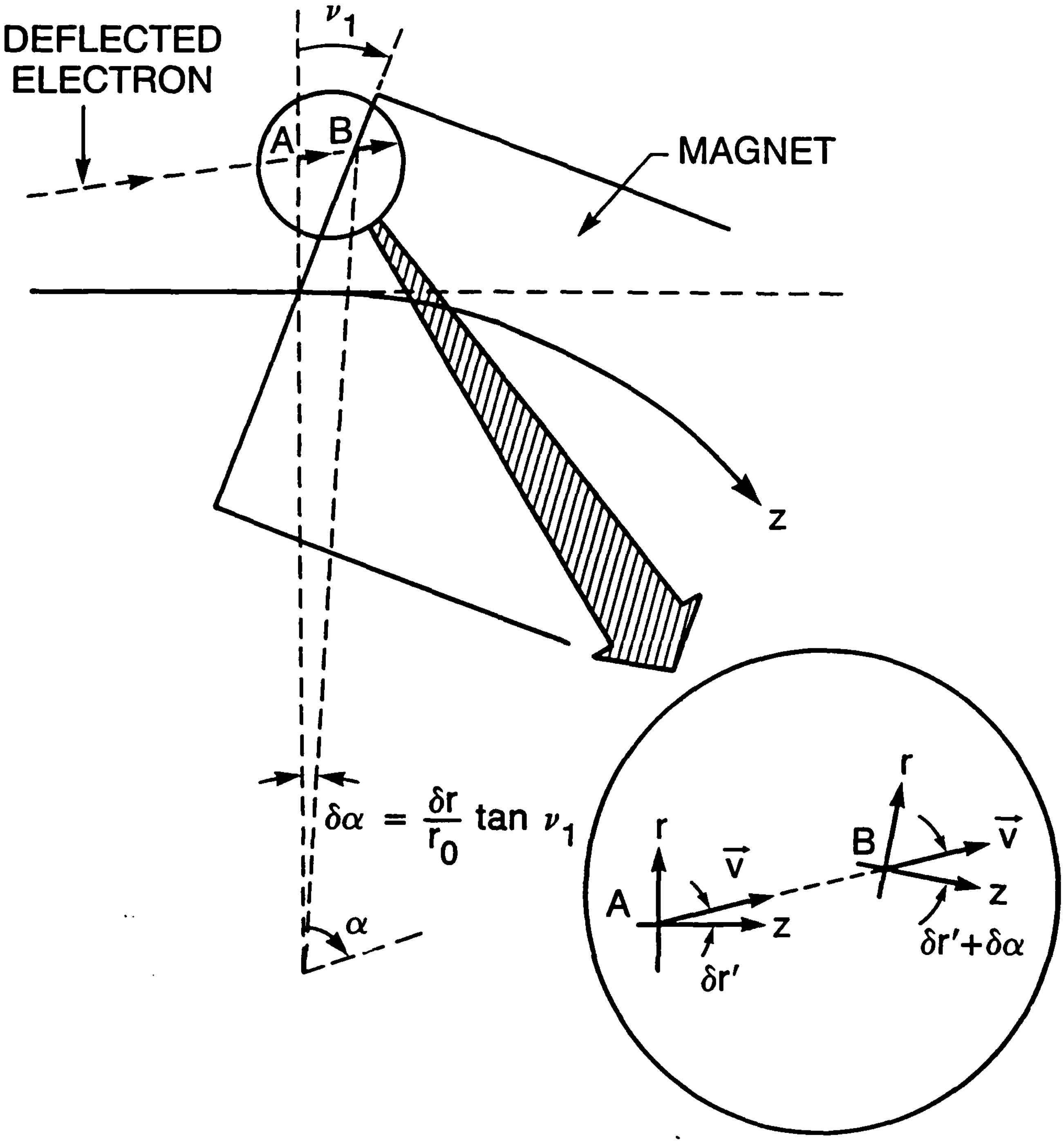

Fig. 2 — Blown-up picture at the magnet entrance. Rotation of the coordinate axis effectively enhances the radial pitch angle